INL/JOU-18-44865-Revision-0

An effective numerical algorithm for intra-granular fission gas release during non-equilibrium trapping and resolution

G. Pastore, D. Pizzocri, C. Rabiti, T. Barani, P. Van Uffelen, L. Luzzi

October 2018

The INL is a U.S. Department of Energy National Laboratory
operated by Battelle Energy Alliance

INL/JOU-18-44865-Revision-0

An effective numerical algorithm for intra-granular fission gas release during non-equilibrium trapping and resolution

G. Pastore, D. Pizzocri, C. Rabiti, T. Barani, P. Van Uffelen, L. Luzzi

October 2018

Idaho National Laboratory
Idaho Falls, Idaho 83415

http://www.inl.gov

Prepared for the
U.S. Department of Energy

Under DOE Idaho Operations Office
Contract DE-AC07-05ID14517

An effective numerical algorithm for intra-granular fission gas release during non-equilibrium trapping and resolution

G. Pastore[a,b,*], D. Pizzocri[c], C. Rabiti[a], T. Barani[c], P. Van Uffelen[d], L. Luzzi[c]

[a] *Idaho National Laboratory, P.O. Box 1625, Idaho Falls, ID 83415-3840, United States*
[b] *Massachusetts Institute of Technology, Department of Nuclear Science and Engineering, 77 Massachusetts Avenue, Cambridge, MA 02139-4301, United States*
[c] *Politecnico di Milano, Department of Energy, Nuclear Engineering Division, via La Masa 34, 20156 Milano, Italy*
[d] *European Commission, Joint Research Centre, Directorate for Nuclear Safety and Security, P.O. Box 2340, 76125 Karlsruhe, Germany*

Abstract

Fission gas release and gaseous swelling in nuclear fuel are driven by the transport of fission gas from within the fuel grains to grain boundaries (intra-granular fission gas release). The process involves gas atom diffusion in conjunction with trapping in and resolution from intra-granular bubbles, and is described mathematically by a system of two partial differential equations (PDE). Under the assumption of equilibrium between trapping and resolution (quasi-stationary approximation) the system can be reduced to a single diffusion equation with an effective diffusion coefficient. Numerical solutions used in engineering fuel performance calculations invariably rely on this simplification. First, we investigate the validity of the quasi-stationary approximation compared to the solution of the general system of PDEs. Results demonstrate that the approximation is valid under most conditions of practical interest, but is inadequate to describe intra-granular fission gas release during rapid transients to relatively high temperatures such as postulated reactivity-initiated accidents (RIA). Then,

*Corresponding author
Email addresses: Giovanni.Pastore@inl.gov (G. Pastore), Davide.Pizzocri@polimi.it (D. Pizzocri), Cristian.Rabiti@inl.gov (C. Rabiti), Tommaso.Barani@polimi.it (T. Barani), Paul.Van-Uffelen@ec.europa.eu (P. Van Uffelen), Lelio.Luzzi@polimi.it (L. Luzzi)

we develop a novel numerical algorithm for the solution of the general PDE system in time-varying conditions. We verify the PolyPole-2 algorithm against a reference finite difference solution for a large number of randomly generated operation histories including prototypical RIA transients. Results demonstrate that PolyPole-2 captures the solution of the general system with a high accuracy and a low computational cost. The PolyPole-2 algorithm overcomes the quasi-stationary approximation and the concept of an effective diffusion coefficient for the solution of the intra-granular fission gas release problem in nuclear fuel analysis.

Keywords: Fission gas, diffusion, trapping, resolution, nuclear fuel modeling, intra-granular fission gas release, quasi-stationary approximation, effective diffusion coefficient, numerical algorithms, modal methods, PolyPole.

---

1. Introduction

The behavior of the fission gases xenon and krypton in oxide nuclear fuel significantly affects the fuel rod thermo-mechanical performance in the reactor. Fission gas retention in the form of bubbles leads to fuel swelling which promotes pellet-cladding mechanical interaction (PCMI), and the concomitant fission gas release (FGR) to the fuel rod free volume increases the rod internal pressure. Moreover, gas release and precipitation in bubbles affect the thermal conductance of the fuel-cladding gap and the fuel thermal conductivity, respectively. Also, beyond a certain burnup the fuel swelling rate increases due to the build-up of gaseous porosity associated with the formation of the sub-micrometric-grain, high burn-up structure (HBS) in both UO_2 [1–5] and MOX [6–9]. Ultimately, the increased fuel gaseous swelling can severely impact the fuel-cladding contact pressure during PCMI [6,8,10–13]. In particular, PCMI is associated with potential safety margin reduction for cladding failure during reactivity-initiated accidents (RIA) in light water reactors [13,14]. Furthermore, considerable FGR has been observed in RIA simulation tests, which would increase cladding loading and the risk of creep-induced cladding rupture by ballooning [6,15].

It follows that accurate models of fission gas swelling and release need to be incorporated in fuel performance codes. In particular, ability to capture peculiarities of fission gas behavior in high-burnup fuel and during rapid power/temperature transients is a requisite in order to evaluate fuel performance during postulated RIA accidents. However, whilst the fission gas behavior in fuel for moderate burnups is fairly well characterised and such understanding is reflected in many models (e.g., [16–23]), modeling of fission gas behavior in high burnup fuel and during transients is still an open issue [3,24–29].

The first and basic stage of FGR and gaseous swelling is gas atom transport from within the grains to grain boundaries (intra-granular fission gas release). This involves thermal and irradiation-enhanced lattice diffusion of single gas atoms in conjunction with trapping in and irradiation-induced resolution from intra-granular bubbles [18,30–35]. The problem is described mathematically by a system of two coupled partial differential equations (PDE), with one equation for the concentration of single gas atoms and one for the gas balance in the bubbles.

The numerical solution of the intra-granular fission gas release problem in time-varying conditions has an enormous practical importance in fuel modeling. In particular, in this work we deal with applications to engineering fuel performance modeling, i.e., the thermo-mechanical analysis of the fuel elements using integral fuel performance codes [36]. In this area of application, the fission gas behavior model is a component of a broader analysis. Also, because of the time and spatial discretization of the problem and the non-linearities involved, an integral fuel performance calculation for a detailed fuel rod irradiation history comprises a very high number of calls of each local model, including the fission gas behavior model. It follows that the numerical solution of the intra-granular fission gas release problem in models applied in integral codes must be computationally efficient, while still guaranteeing a suitable accuracy. Of course, the numerical solution may be obtained using standard space-discretization methods such as finite difference schemes. However, the associated high computational cost makes standard solution techniques impractical for application in integral

fuel performance codes [32,37].

Speight [30] derived the concept of an effective diffusion coefficient embodying the effects of trapping and resolution, which reduces the problem of intra-granular fission gas release to a single diffusion equation. Such a simplified formulation can be applied to time-varying conditions under the assumption of instantaneous equilibrium between trapping and resolution (quasi-stationary approximation). Numerical algorithms have been developed in the past that provide solutions of the simplified problem at high speed of computation for application in engineering calculations [17,37–44]. In this connection, the authors recently developed an improved numerical algorithm called PolyPole-1 [45]. Speight's simplified formulation is generally adopted for models employed in integral fuel performance codes (e.g., [46–50]). To the best of the authors' knowledge, no numerical algorithm has been developed yet that is able to solve the general system of PDEs at low computational cost. The development of such an algorithm is an open issue and simply prevents the inclusion of generally valid fission gas behavior models in integral codes [32,51].

In this paper, first, we investigate the validity of the quasi-stationary approximation by comparison to the solution of the general system of PDEs. Then, we develop a novel algorithm to numerically solve the general system of PDEs at low computational cost. The new algorithm extends the PolyPole-1 concept, and is called PolyPole-2.

The outline of the paper is as follows. In Section 2, we discuss the mathematical formulation of the intra-granular fission gas release problem. In Section 3, we investigate the validity of the quasi-stationary approximation relative to the system of coupled PDEs that is the general formulation of the problem. In Section 4, we present the concept of the PolyPole-2 algorithm for the effective solution of the general system of PDEs. In Section 5, we verify the PolyPole-2 algorithm through comparisons to accurate finite-difference reference solutions for a large number of randomly generated operation histories covering both operational conditions and postulated RIAs. Conclusions are drawn in Section 6.

2. Mathematical problem

The problem of intra-granular fission gas release can be stated mathematically with the following system of PDEs (e.g., [18,30])

$$\begin{cases} \frac{\partial c}{\partial t} = D\nabla^2 c - gc + bm + \beta \\ \\ \frac{\partial m}{\partial t} = +gc \qquad - \qquad bm \end{cases} \tag{1}$$

where c (at·m^{-3}) is the concentration of single gas atoms dissolved in the lattice, m (at·m^{-3}) the concentration of gas atoms in intra-granular bubbles, t (s) the time, D (m^{2}s^{-1}) the single gas atom diffusion coefficient, g (s^{-1}) the trapping rate of gas atoms at bubbles, b (s^{-1}) the rate of irradiation-induced gas atom resolution from bubbles back into the lattice, and β (at·m^{-3}s^{-1}) the gas generation term.[1]

[1] An empirical expression for the diffusion coefficient, D, due to Turnbull et al. [35] is

$$\begin{aligned} &D = D_1 + D_2 \\ &D_1 = 7.6 \times 10^{-10}\, exp\left(-\, 4.86 \times 10^{-19}/(kT)\right) \\ &D_2 = 1.41 \times 10^{-25}\, \sqrt{F}\, exp\left(-\, 1.91 \times 10^{-19}/(kT)\right) \end{aligned} \tag{2}$$

where D_1 (m^{2}s^{-1}) represents intrinsic thermal diffusion, D_2 (m^{2}s^{-1}) represents irradiation-enhanced diffusion, F (m^{-3}s^{-1}) is the fission rate and k (JK^{-1}) the Boltzmann constant. Based on Ham's [52] theory for diffusion-limited precipitation at spherical particles, the trapping rate, g, can be calculated as

$$g = 4\pi DRN \tag{3}$$

where R (m) the mean radius of intra-granular bubbles and N (m^{-3}) the bubble number density. Various theories have been proposed for the mechanisms of resolution [18,53–56]. An expression often adopted for the resolution rate, b, is the one from [18], which is a slight modification of Turnbull's [55]

$$b = 3.03F\pi l_f\, (R + Z_0)^2 \tag{4}$$

where l_f (m) the length of a fission fragment track and Z_0 (m) the radius of influence of a fission fragment track. The generation rate of fission gas is calculated as

$$\beta = YF \tag{5}$$

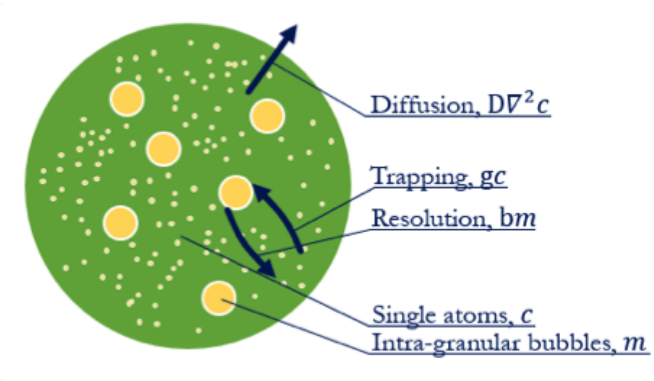

Figure 1: Sketch representing the mechanisms involved in intra-granular fission gas release.

Eqs. 1 represent the intra-granular fission gas release problem as gas atom diffusion (term $D\nabla^2 c$) in conjunction with trapping (gc) in and resolution (bm) from intra-granular bubbles. The second of Eqs. 1 represents the balance of the gas in bubbles. Single gas atom diffusion is responsible for gas transport to grain boundaries (intra-granular fission gas release). The processes described by Eqs. 1 are represented in Fig. 1.

Note that more detailed formulations of the problem are possible that include terms of bubble mobility (e.g., [22,57,58]), bubble nucleation (e.g., [22,59]), up to cluster dynamics models that track the full distribution of bubble sizes and potentially also consider interactions between species (atom trapping to bubbles but also bubble to bubble interactions, i.e., coalescence) as well as Brownian and drift diffusion of each species (e.g., [60]). Cluster dynamics models can be used to inform reduced-parameter engineering models (such as Eqs. 1). Indeed, they require dedicated codes and high performance computing power. In this work, we consider the formulation of the intra-granular fission gas release problem

where Y (/) is the total yield of fission gas atoms. Hence, in general, the parameters of Eqs. 1 vary in time as temperature and power (fission rate) vary during irradiation. In particular, D and g present rapid variations during transients owing to to their exponential dependence on the temperature.

expressed by Eqs. (1). This is the simplest form that includes explicitly the effects of trapping and resolution, whose consideration is the main focus of the present work. Extension of the work to more complex formulations is of interest in perspective.

A further assumption that is generally adopted is that of spherical grain geometry. The analytic modal solution of Eqs. 1 in spherical geometry for constant conditions (i.e., constant D, g, b, β) is

$$\begin{cases} c(r,t) = \frac{1}{\sqrt{2\pi a}} \sum_{n=1}^{\infty} \frac{\sin(\lambda_n r)}{r} \left[A_n \exp(-p_n t) + B_n \exp(-q_n t) + C_n\right] \\ m(r,t) = \frac{1}{\sqrt{2\pi a}} \sum_{n=1}^{\infty} \frac{\sin(\lambda_n r)}{r} \left[A'_n \exp(-p_n t) + B'_n \exp(-q_n t) + C'_n\right] \end{cases} \tag{6}$$

where a is the radius of the spherical grain, n is the mode index, λ_n are the eigenvalues of the radial part of the spherical Laplacian with Dirichlet boundary condition $(c, m)(r = a, t) = 0$ and symmetry condition $\partial(c, m)/\partial r|_{r=0} = 0$, p_n and q_n are the poles of the solution and A, B, C are the time coefficients. The complete derivation of Eqs. 6 and the expressions for the poles and time coefficients are provided in Appendix A. In realistic problems, the parameters in Eqs. 1 vary in time (foonote 1), so that this solution is not directly applicable to fuel performance calculations. Hence the need for algorithms to numerically solve the mathematical problem for time-varying conditions.

Speight [30] derived the analytic modal solution of Eqs. 1 in spherical geometry for constant conditions and with zero initial conditions for c and m. He then simplified the solution assuming that the rates of trapping and resolution are high compared to the rate of diffusion to grain boundaries. Under this assumption, the condition of equilibrium between trapping and resolution, or stationary condition,

$$\frac{\partial m}{\partial t} = +gc - bm = 0 \tag{7}$$

is reached rapidly compared to the time scale of diffusion. Eq. 7 corresponds to the concentrations c and m having reached an equilibrium ratio $c/m =$

b/g. Speight showed that the fractional gas release to the grain boundaries under the above assumption is analogous to the expression derived previously by Booth [61] for diffusion in the absence of trapping/resolution, but with the gas atom diffusion coefficient, D, substituted by an effective diffusion coefficient, $D_{eff} = b/(b+g)\ D$. The correction of the diffusion coefficient accounts for the reduced apparent diffusion as part of the gas is trapped into immobile bubbles.

Intuitively, if g and b are constant and if gas diffusion to the grain boundaries is neglected (which is a condition approached if diffusion is slow compared to trapping and resolution), after sufficient time the gas concentrations m and c will approach an equilibrium ratio (Eq. 7). White and Tucker [18] noted that combining Eqs. 1 and 7, and writing the total gas concentration as $c_t = c + m$, Eqs. 1 can be directly reduced to

$$\frac{\partial c_t}{\partial t} = D_{eff} \nabla^2 c_t + \beta \tag{8}$$

which is the equation for pure diffusion with the effective diffusion coefficient of Speight (and referred to as Speight's formulation henceforth). A detailed derivation of Speight's formulation is given in Appendix B.

The so-called quasi-stationary approximation applies to time-varying conditions and refers to considering that m evolves with a succession of equilibrium states so that the condition expressed by Eq. 7 is verified at any time. This assumption implies that Eq. 8 is valid for time-varying conditions as well. Thus, the quasi-stationary approximation is effectively an extension of Speight's concept to time-varying conditions. However, the quasi-stationary approximation and Speight's formulation are generally referred to alike in the literature. In the remainder of the paper, we also refer to them alike for practical reasons.

Note that derivation of Eq. 8 requires the additional assumption that parameters b and g are uniform in space across the domain (grain). Veshchunov and Tarasov [51] noted that because the trapping rate, g, depends linearly on the concentration c of dissolved gas (foonote 1), this latter assumption is effectively an inconsistency as it implies that $c(r)$ is uniform in space (c being subject to Fickian diffusion, it cannot be considered as uniform in general).

Efficient numerical algorithms for the solution of Eq. 8, in time-varying conditions have been developed (see, e.g., [37,41,45]). Accordingly, this simplified formulation is universally adopted for models employed in integral fuel performance codes (e.g., [46–50]). To the best of the authors' knowledge, no algorithms for the solution of the general system, Eqs. 1, efficient enough to be used effectively in integral codes are available [32,45].

3. Validity of the quasi-stationary approximation

The concept of the quasi-stationary approximation is illustrated in graphical form in Fig. 2. The general problem, expressed by Eqs. 1 and represented in Fig. 2a, explicitly describes the time evolution of both concentrations of gas atoms in solution (c) and in bubbles (m) with two differential equations. Both the diffusion and trapping/resolution components are explicitly included and act simultaneously in affecting the gas concentrations. Diffusion only affects the concentration c (in consequence of the hypothesis of immobile bubbles) while trapping/resolution affect both c and m. Because trapping and resolution counteract each other, the ratio of concentrations tends to an equilibrium condition (Eq. 7). However, in the general non-stationary situation, the ratio of

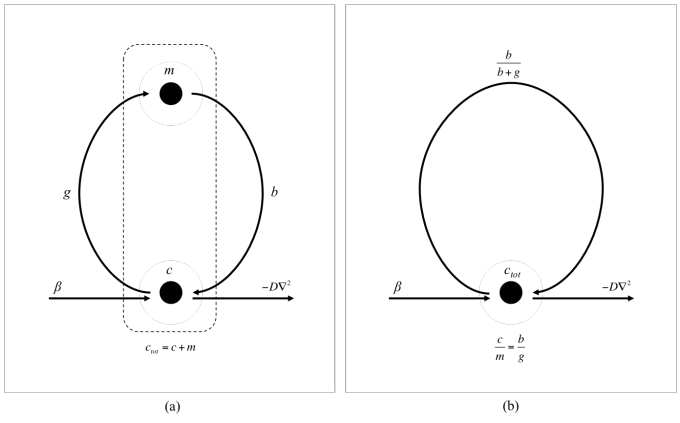

Figure 2: Graphical representation of (a) the general formulation of the intra-granular fission gas release problem and (b) Speight's formulation.

concentrations can depart from equilibrium. The system will be in such a non-equilibrium condition following a change in the trapping and/or resolution rates (g and b, respectively) so that the instantaneous c/m ratio no longer satisfies Eq. 7 and concentrations move towards a new equilibrium. The time for this transition is finite. During the non-equilibrium period, the diffusion operator acts on a concentration $c \neq (b/g)\, m$. Under the quasi-stationary approximation, c and m are at the equilibrium ratio at any time. Hence, the fraction of the total gas concentration affected by diffusion is at any time $c = b/(b+g)\; c_t$ (Eq. 8 and Fig. 2b). The idea of the quasi-stationary approach is that the transition between states of equilibrium is fast compared to diffusion, hence, the assumption of instantaneous equilibrium does not lead to a significant error in the calculated intra-granular fission gas release.

In his review of intra-granular fission gas behavior, Lösönen [32] performed an investigation of the validity of Speight's formulation by solving the general system, Eqs. 1, using a finite-difference scheme and comparing results to Speight's solution. Considering a rectangular initial profile for the gas concentration and applying a sudden increase of the diffusion coefficient at the beginning of the calculation, he showed that during the subsequent time under constant irradiation conditions, Speight's solution significantly departed from the solution of the general system. On this basis, he identified the adoption of Speight's formulation as a major weakness of fission gas models used in fuel performance codes. However, in this study Lösönen made an assumption of constant gas concentration in bubbles, m (and constant bubble radius) when applying Speight's formulation. Indeed, the quasi-stationary approach rather implies that m evolves with a succession of equilibrium states. This does not imply by any means that m is constant over time but only that it adjusts instantaneously to a change in the conditions so that equations can be decoupled.

Here, we perform another investigation of the validity of the quasi-stationary approximation. We solve both the general system, Eqs. 1, and Speight's formulation, Eq. 8, using identical values for the parameters in either case. We developed highly accurate finite difference (FD) algorithms for the numerical

solution of both formulations with time-varying parameters. For more details on the FD algorithms, see Section 5.1. For these calculations, the algorithms have been coded in a stand-alone computer program. Although Speight's formulation turns out to be an excellent approximation of the general problem for most situations of practical interest, as shown in Section 5.3, we found it failing to describe transients to relatively high temperatures occurring at the scale of milliseconds. In terms of reactor conditions of practical interest, these correspond to postulated RIA transients. Hereafter, we demonstrate this circumstance for an exemplifying case. An extensive numerical experiment that substantiates the conclusion is described in Section 5.2.

As a prototypical RIA transient, we consider the CABRI REP-Na 5 power pulse experiment [6,62]. During the experiment, a UO_2/Zircaloy-4 fuel rodlet was transient-tested with a Gaussian-type power pulse. Full width at half maximum (FWHM) of the power pulse was 8.8 ms. The analysis considers a location close to pellet periphery. Time-dependent specific power and temperature are taken from [25] and are input for the analysis. Time-dependent parameters are calculated as functions of power (fission rate) and temperature (see footnote 1 for dependencies). Using the aforementioned FD algorithms we solve the intragranular fission gas release problem over time for both Eq. 8, which implies the quasi-stationary approximation, and the general problem, Eqs. 1. We consider a constant grain radius $a = 0.15$ μm. This value is typical of UO_2 HBS and smaller than typical grain radii in the regular fuel structure. (See Section 5.2 for an investigation of the effect of the grain size). The analysis is presented in Fig. 3. The power pulse induces a rapid temperature transient that reaches a temperature $T > 2500$ K over tens of milliseconds, and is followed by a cooling transient that lasts a few hundreds of milliseconds (Fig. 3, top graph).

The heating transient leads to an increase in the gas atom diffusion coefficient, D (therefore, in the trapping parameter, g – see footnote 1). The equilibrium ratio of concentrations, $c/m = b/g$, is correspondingly reduced. Consequently, c decreases in favor of m to restore equilibrium, by virtue of the second of Eqs. 1. As shown in Fig. 3 (second graph from top), the concentra-

Figure 3: Power and temperature histories for the REP Na-5 power pulse test (top) and calculation results. Both solutions for the general formulation and the quasi-stationary approximation were obtained using accurate finite difference algorithms.

tion of single gas atoms, c, calculated under the quasi-stationary approximation decreases to effectively zero during the heating transient and increases during

the cooling transient to follow the equilibrium curve. Because the trapping and resolution rates are finite, there is actually a kinetic effect, with concentrations departing from equilibrium. This behavior is captured by the solution of the general system, which is also shown in the figure.

We define an equilibrium non-dimensional group, E, as

$$E = \frac{gc}{bm} \tag{9}$$

During equilibrium between trapping and resolution, Eq. 7 is verified so that $E = 1$. The departure of E from 1 gives a measure of the departure of the system from equilibrium. As shown in Fig. 3 (third graph from top), the system reaches $E > 10^5$ during the transient considered here. It follows that under the quasi-stationary approximation, diffusion acts on a concentration c that is under-estimated during the non-equilibrium period following a heating transient and consequently, intra-granular fission gas release is under-estimated. During a rapid transient to high temperature, where departure from equilibrium is strong and at the same time, the diffusion rate is high, the effect can be significant. This is illustrated in the bottom plot of Fig. 3, showing that a significant intra-granular fission gas release is calculated when solving the general system but is almost completely neglected if the quasi-stationary approximation is applied.

Based on this study, we conclude that while the quasi-stationary approximation holds for most situations of practical interest, for rapid transients to high temperatures occurring at the scale of milliseconds, such as postulated RIA transients, the approximation becomes inadequate.

4. PolyPole-2 algorithm

The authors previously presented the development of the PolyPole-1 algorithm for the solution of Speight's formulation (Eq. 8) in time-varying conditions [45]. Here, we present a new numerical algorithm for the solution of the general intra-granular fission gas release problem (Eqs. 1) in time-varying conditions. This new algorithm is effectively a generalization of PolyPole-1, and is called PolyPole-2.

Similar to PolyPole-1, the development of the new algorithm requires in the first place knowledge of the analytic modal solution of the mathematical problem in spherical geometry for constant conditions (i.e., constant parameters D, g, b, β). Speight [30] derived the analytic modal solution of Eqs. 1 with zero initial conditions for c and m. The more general solution for nonzero initial conditions is needed here, because the algorithm is applied at each time step in a fuel performance calculation with the initial conditions being given at the beginning of the time step. We derive the analytic modal solution of Eqs. 1 in spherical geometry for constant parameters and with nonzero initial conditions for c and m. The complete derivation is provided in Appendix A. The new numerical algorithm is described hereafter.

We seek an approximate solution, for time-varying parameters, of Eqs. 1 re-written in vectorial form as

$$\frac{\partial}{\partial t}u = (\mathbf{D} + \mathbf{E})u + s \tag{10}$$

where $u = [c\ m]$ and $s = [\beta\ 0]$ are vectors of the gas concentrations and the source term, respectively. The diffusion $\mathbf{D}$ and exchange $\mathbf{E}$ operators are defined as

$$\mathbf{D} = \begin{bmatrix} D\nabla^2 & 0 \\ 0 & 0 \end{bmatrix} \tag{11}$$

$$\mathbf{E} = \begin{bmatrix} -g & +b \\ +g & -b \end{bmatrix} \tag{12}$$

The boundary conditions of Eq. 10 are $u(r = a, t) = 0$ and $\partial u/\partial r|_{r=0} = 0$. The initial condition is $u(r, t = 0) = u_0(r) = [c_0(r)\ m_0(r)]$.

Note that by replacing in Eq. 10 the diffusion-exchange operator $(\mathbf{D} + \mathbf{E})$ by $Db/(b + g)\nabla^2$, the source vector s by β and u by $c_t = c + m$, Eq. 10 reduces to Eq. 8. The notation of Eq. 10 thus effectively reduces Eqs. 1 to the same form as Eq. 8. This highlights that the new PolyPole-2 algorithm for the solution of Eq. 10 is a generalized case of the PolyPole-1 algorithm for the solution of Eq. 8.

We seek an approximate solution u^* of Eq. 10 for the case of time-varying $(\mathbf{D}+\mathbf{E})$ and s. We make the *ansatz* that the solution can be approximated with the following modal expansion

$$u^*(r,t) \approx \sum_{n=1}^{\infty} z_n^*(t)\psi_n(r) \tag{13}$$

The time coefficients, $z_n^*(t)$, contain the information about the time dependence of the approximate solution (i.e., the characteristic poles of the system). The spatial modes of the approximate solution, $\psi_n(r)$, are taken the same as the spatial modes of the analytic solution for constant conditions (see Appendix A).

Another fundamental assumption of the PolyPole concept is that the time coefficients of the approximate solution, $z_n^*(t)$, may be expressed as the time coefficients of the analytic solution for constant conditions, $z_n(t)$ (Appendix A), multiplied by an operator $\mathbf{P}_n$ that embodies the information on the deviation from constant conditions. Thus, we write

$$z_n^*(t) = \mathbf{P}_n z_n(t) \tag{14}$$

The operator $\mathbf{P}_n$ is applied to each mode of the solution. The formulation for this operator is comprised of two distinct polynomials of order J

$$\mathbf{P}_n = \begin{bmatrix} 1+\sum_{j=1}^{J} p_j dt^j & 0 \\ 0 & 1+\sum_{j=1}^{J} q_j dt^j \end{bmatrix} \tag{15}$$

This definition of $\mathbf{P}_n$ is consistent with the polynomial correction factor used in the PolyPole-1 algorithm [45]. In this way, the problem of finding an approximate solution for time-varying conditions is shifted to the problem of finding the coefficients of the polynomials in $\mathbf{P}_n$. To calculate the polynomial coefficients, p_j and q_j, $2J$ equations are needed. This set of equations is obtained by sampling the time-varying operators, $\mathbf{D}(t)$, $\mathbf{E}(t)$ and $\mathbf{S}(t)$, at J uniformly distributed instants along the time-step dt. The sets of sampled values, $\mathbf{D}[j]$, $\mathbf{E}[j]$ and $\mathbf{S}[j]$, contain the information on the variation of the operators along the time step and are used to calculate the corrective polynomials, as follows.

The time coefficients $z^*(t)$ defined by Eq. 14 are assumed to satisfy Eq. 28 (Appendix A) at the sampling times $t[j]$, $t_i \leq t[j] \leq t_{i+1}$. In vector notation:

$$\left.\frac{\partial(\mathbf{P}_n z_n)}{\partial t}\right|_{t[j]} = -\mathbf{\Lambda}_n[j]\mathbf{P}_n z_n + \langle \psi_n | s[j] \rangle \tag{16}$$

where we applied the scalar product defined by Eq. 27 and $\mathbf{\Lambda}_n$ is an operator defined as

$$\mathbf{\Lambda}_n = \begin{bmatrix} \frac{Dn^2\pi^2}{a^2} + g & -b \\ -g & +b \end{bmatrix} \tag{17}$$

Eq. 16 defines a linear system of $2J$ equations for the polynomial coefficients p_j and q_j. The time coefficients of the analytic solution for constant conditions, z_n, are calculated through Eqs. 31, with parameters taken as averages of the sampled values $\mathbf{\Lambda}_n[j]$ and $S[j]$ along the time step.

The spatial modes, $\psi_n(r)$, are calculated as per Eq. 25. The PolyPole-2 solution is then reconstructed as a linear combination of the spatial modes with the corrected time coefficients, according to Eqs. 13 and 14. The series is approximated by a finite number of terms (N, number of modes). The value of N is determined based on a D'Alembert remainder criterion identical to that used for PolyPole-1 [45].

Similar to PolyPole-1, the newly developed PolyPole-2 algorithm combines the physical poles of the analytic solution and a polynomial correction to account for the time dependence of the coefficients. The idea behind the PolyPole concept is that the spatial dependence of the solution for time-varying conditions can be approximated by the spatial dependence of the solution for constant conditions, which is known analytically. The deviation from constant conditions is fully embodied in the time-dependent part of the solution and approximated by the time coefficients of the solution for constant conditions multiplied by an appropriate correction. Exploiting an analytic representation of the spatial dependence avoids using spatial discretization and therefore allows for significantly lower computational time compared to spatial discretization methods such as FD schemes. In view of this concept, the algorithm may be labeled as semi-analytic.

5. Verification

In this Section, we verify the PolyPole-2 solution against accurate reference solutions for both RIA conditions and operational conditions through an extensive numerical experiment.

5.1. Setup of the numerical experiment

The numerical experiment consists of the application of the PolyPole-2 algorithm to the numerical solution of Eqs. 1 for a large number of randomly generated histories. The results from the PolyPole-2 algorithm are compared to a high-accuracy finite-difference reference solution. This FD algorithm is fully implicit first order in time and second order in space. An adaptive time step control is included, based on the estimation of the second-order error calculated as the difference between the explicit and implicit solutions [63].[2] The adaptive time stepping scheme ensures that the second-order error of the FD solution is always lower than a prescribed tolerance. For this numerical experiment, we set the tolerance of the reference FD algorithm to 10^{-6}. A more detailed description of the method is given in [45]. Note that relative to [45], we extended the FD algorithm to the solution of Eqs. 1.

For these calculations, the algorithms have been coded in a stand-alone computer program. The random histories, both for RIAs and operational conditions, are in terms of temperature and fission rate. From the input time-dependent temperature and fission rate, the program calculates the time-dependent parameters[3] in the diffusion and exchange operators, $\mathbf{D}(t)$ and $\mathbf{E}(t)$, and in the source term, s (Section 4). Then, the program computes the solution of the

[2]The explicit scheme is applied at each time step with the only purpose of estimating the second-order error. The reference solution is calculated by application of the implicit scheme.

[3]We use the expressions for the diffusion coefficient, D, by Turnbull et al. [35], the resolution rate, b, by White and Tucker [18], the trapping rate, g, by Ham [52], and a value of 0.3 for the total yield of fission gas atoms. See also footnote 1. For the purpose of this numerical experiment, as long as values and dependencies are realistic, the specific choices are arbitrary.

intra-granular fission gas release problem with both the reference FD and the PolyPole-2 algorithms.[4]

The figure of merit chosen for the verification of the numerical solution is the fractional intra-granular fission gas release at the end of each history, defined as

$$f = \frac{\bar{c}_{created}(t_{end}) - \bar{c}(t_{end}) - \bar{m}(t_{end})}{\bar{c}_{created}(t_{end})} \tag{18}$$

where $\bar{c}_{created}(t_{end})$ (at·m^{-3}) is the integral of $\beta(t)$ from 0 to the final time of each random history, t_{end}.

5.2. RIA conditions

In order to verify the PolyPole-2 algorithm for RIA transients, we considered 500 histories randomly generated within a range of realistic RIA conditions. Ranges were determined based on the sensitivity study from Jernkvist [64]. In particular, the RIA random histories have the following characteristics:

- The FWHM of the power pulse, τ_{RIA}, is a random variable, sampled uniformly in the range 20–60 ms.
- The total specific energy injected, E_{RIA}, is a random variable, sampled uniformly in the range 400–800 J·$(\mathrm{g_{UO_2}})^{-1}$.
- The maximum specific power reached, P_{RIA} (W·g^{-1}), is calculated as $P_{\mathrm{RIA}} = 62.5 \cdot E_{\mathrm{RIA}}/\tau_{\mathrm{RIA}}$ [25].
- The power pulse shape is calculated according to the Nordheim-Fuchs model [25].
- The initial temperature, T_0 (K), is calculated as $T_0 = 883 \cdot (5 \cdot 10^{-4} E_{\mathrm{RIA}} + 0.7772)$ (uniform in the range 863–1039 K). This correlation is derived from the results of the RIA sensitivity analysis from [64].

[4] For this numerical experiment, we use second-order corrective polynomials (i.e., $J = 2$ in Eq. 15) in PolyPole-2. Also, we use a limiting value of 10^{-7} for the D'Alembert remainder.

- The maximum temperature reached, T_{max} (K) is calculated as $T_{max} = 2564 \cdot (5 \cdot 10^{-4} E_{\mathrm{RIA}} + 0.7772)$ (uniform in the range 2506–3017 K) [64].
- The maximum temperature is reached after $2\tau_{\mathrm{RIA}}$. The temperature increase in time is calculated based on the integral of the power pulse.
- The final time is fixed at 300 ms.
- The final temperature, T_{end} (K), is calculated as $T_{end} = 1227 \cdot (5 \cdot 10^{-4} E_{\mathrm{RIA}} + 0.7772)$ and is sampled uniformly in the range 1200–1444 K [64].

In addition, prior to the RIA transient a period of 100 hours at constant temperature T_0 is considered, in order to establish the condition of equilibrium between trapping and re-solution before the transient begins.

In the study we also consider the effect of grain size. In particular we consider two values for the grain radius, i.e., (1) a value of 5 μm that is typical for the regular structure of oxide fuel and (2) a value of 0.15 μm that is representative of the high burnup structure (e.g., [4,5]).[5] We divide the 500 random histories for this numerical experiment into two subsets of 250 histories each. The two subsets differ by the considered grain size. The value of the grain radius is time-independent during the calculations. This is for simplicity and in order to isolate the solution of the intra-granular fission gas release mathematical problem from other effects such as grain growth or recrystallization. Note that the PolyPole algorithms are also applicable to problems with time-varying grain size in fuel performance calculations.

As for the initial conditions at the beginning of the simulation, for the calculations with a grain radius of 5 μm we consider an initial gas concentration

[5] In fact it remains to be ascertained whether the mechanisms of intra-granular FGR in the HBS are analogous to the regular fuel structure. Some experiments indicated that the small grains of the HBS in the examined samples were depleted of intra-granular defects and gas bubbles [65], or that the density of intra-granular bubbles was much lower than that found in the regular fuel structure [66]. However, other experiments demonstrated the presence of a high density of intra-granular HBS bubbles [67]. This is worth further investigation in future studies of fission gas behavior in the HBS.

corresponding to the gas generated during an irradiation up to 50 GWd/t. All gas is assumed to be stored in the grains initially. For the calculations with a grain radius of 0.15 μm, the initial concentration is set to 10^{26} at·m^{-3}, which corresponds approximately to the asymptotic gas concentration achieved in the HBS grains [68]. As for the gas distribution, for both sets of simulations we consider 70% of the gas in solution and 30% in bubbles, initially [18]. For equilibrium between trapping and resolution (Eq. 7), this corresponds to a ratio $b/(b+g) = 0.7$, which is realistic for typical values of the resolution and trapping rates.

The results of the numerical experiment are presented in Fig. 4 on a linear scale. Each data point in this figure corresponds to one of the randomly generated operation histories and represents the intra-granular fission gas release (Eq. 18) obtained with the PolyPole-2 algorithm versus the reference FD solution. The deviation from the 45° line is a measure of the accuracy of PolyPole-2.

Results appear to be distributed between two clusters of data points. The higher intra-granular fission gas release results (5–15%, approximately) correspond to the simulations with the smaller grain radius equal to 0.15 μm. With a small grain radius diffusion to grain boundaries occurs at a higher rate (considering a pure diffusion problem as a first approximation, the diffusion rate is $\sim D/a^2$), thus leading to higher intra-granular fission gas release compared to behavior with larger grains. These results indicate that the PolyPole-2 and reference solutions are very close for all of the 250 random histories in this subset of calculations. In Fig. 4, we also show the results from the FD solution of Eq. 8 (which implies the quasi-stationary approximation) for the same input histories. Results demonstrate that the quasi-stationary approximation is inadequate to describe the fast transients to relatively high temperatures (RIAs) considered in this study. In particular, the approximation leads to a strong (nearly 100%) under-prediction of the higher intra-granular fission gas release values.

Results are presented in Fig. 5 on a logarithmic scale. It is confirmed that the PolyPole-2 algorithm calculates the solution of the general system of PDEs with very good accuracy. Again, the clusters of data points at higher intra-

Figure 4: Linear-scale comparison between intra-granular fission gas release calculated by the PolyPole-2 algorithm and the reference FD algorithm for the general PDE system. The corresponding FD solutions for the quasi-stationary approximation are also included. Each data point corresponds to a calculation with randomly generated RIA conditions.

granular fission gas release refer to the simulations with the smaller grain radius of 0.15 μm. It becomes apparent that also for the simulations with the larger grain radius of 5 μm, results under the quasi-stationary approximation are significantly under-predicted. However, intra-granular fission gas release for this set of simulations is lower. This is due to a larger grain size which is associated with a lower gas diffusion rate. In particular, values of $\approx$0.1-0.3% are calculated, which are of the order of the total FGR during a typical base irradiation. Note that the accuracy of the PolyPole-2 algorithm in this region can be further improved by considering a higher number of modes in the series expansion, i.e., by tightening the tolerance in the D'Alembert remainder criterion. Again, under the quasi-stationary approximation intra-granular fission gas release is effectively neglected.

Besides accuracy, speed of computation is an essential feature for an algo-

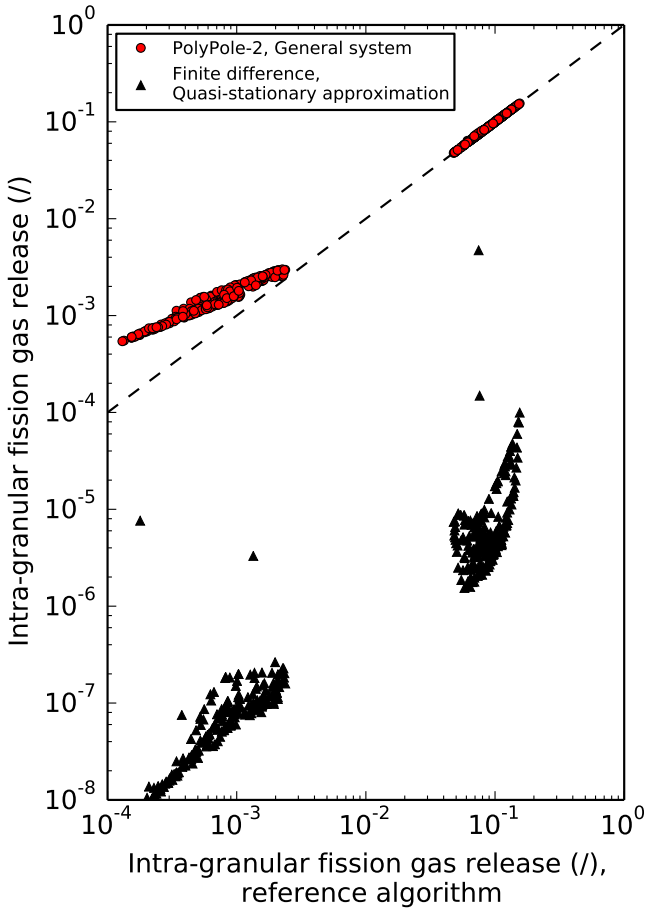

Figure 5: Logarithmic-scale comparison between intra-granular fission gas release calculated by the PolyPole-2 algorithm and the reference FD algorithm for the general PDE system. The corresponding FD solutions for the quasi-stationary approximation are also included. Each data point corresponds to a calculation with randomly generated RIA conditions.

rithm to be effectively employed in an integral fuel performance code. The computational times (i.e., the time taken for each simulation) for the PolyPole-2 and FD algorithms are compared in Fig. 6. The computational time associated with the PolyPole-2 algorithm is approximately two orders of magnitude lower than that associated with the FD algorithm. The computational time of PolyPole-2

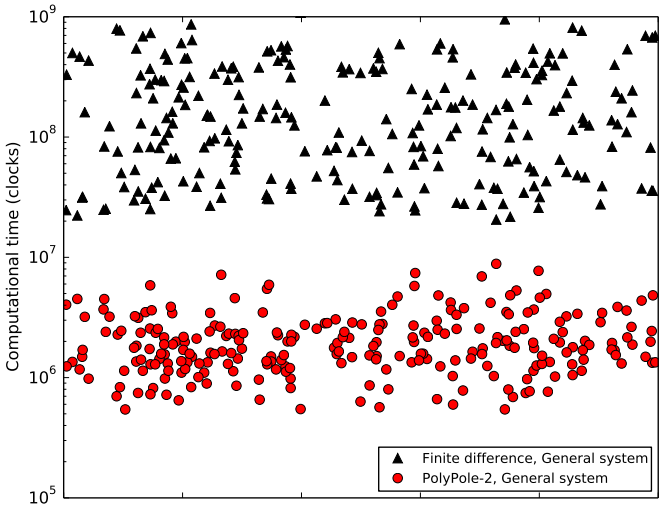

Figure 6: Comparison between the computational times associated with the FD and PolyPole-2 algorithms for the solution of the general PDE system. Each data point corresponds to a calculation with randomly generated RIA conditions.

is roughly two times higher than that of PolyPole-1[6], which in turn is in line with state-of-the-art algorithm used in fuel performance codes, as demonstrated in [45]. Such efficiency of computation, combined with the demonstrated accuracy, makes PolyPole-2 suitable for implementation in any fuel performance code.

5.3. Operational conditions

The verification of the PolyPole-2 algorithm for RIA transients presented in Section 5.2 confirms that PolyPole-2 provides an accurate solution for conditions where solving the general PDE system to capture non-equilibrium behavior is of significance compared to the quasi-stationary approximation. In this Section, we verify PolyPole-2 also for operational conditions, where the quasi-stationary

[6]This appears consistent with the fact that a double amount of operations is required for PolyPole-2 to solve the two-equation system relative to the single-equation solution of PolyPole-1

approximation is valid, in order to confirm its general applicability. The numerical experiment for this comparison is comprised of 1000 randomly generated operation histories with the following characteristics

- Each individual history is piecewise-linear with varying temperature and fission rate.
- In each individual history, the following quantities are considered as random variables (sampled from uniform distributions):
  - number of linear steps (1−50);
  - time duration of each linear steps (0−1000 h);
  - temperature (300−2700 K);
  - fission rate ($0-3 \cdot 10^{19}$ fiss m^{-3} s^{-1}).

Using accurate finite difference algorithms for both the quasi-stationary and general formulations, we have separately verified that for these operational conditions the difference between solutions obtained with the two formulations is negligible and thus the quasi-stationary approximation is valid. The PolyPole-1 algorithm previously developed by the authors has been indipendently verified to provide an accurate solution to the problem in this case [45]. Clearly, the quasi-stationary approximation is a particular case of the general formulation and under conditions where the approximation is valid, PolyPole-2 must closely match the PolyPole-1 solution. The results of the numerical experiment are presented in Fig. 7. Each data point in these figures corresponds to one of the randomly generated operation histories and represents the intra-granular fission gas release (Eq. 18) obtained with the PolyPole-2 algorithm versus the reference (PolyPole-1) solution. Results indicate that the solutions are very close for all of the 1000 random histories considered and therefore the PolyPole-2 solution correctly reduces to the quasi-stationary solution for operational conditions.

Figure 7: Comparison between the values of intra-granular fission gas release calculated with the PolyPole-2 and the PolyPole-1 algorithms. Each data point corresponds to a calculation with randomly generated operational conditions.

6. Conclusions

In this paper, first, we presented an investigation of the quasi-stationary approximation adopted in the calculation of intra-granular fission gas release in current fuel performance codes. Results demonstrated that the approximation is valid for most situations of practical interest, but is inadequate to model intra-granular fission gas release during rapid transients to relatively high temperatures such as postulated RIA accidents. Second, to overcome the quasi-stationary approximation, we developed a novel algorithm to numerically solve the general system of coupled PDEs in time-varying conditions at low computational cost. This new algorithm, called PolyPole-2, is based on the analytic modal solution of the PDE system for constant conditions, with the addition of polynomial corrective terms that embody the information on the deviation from constant conditions. We verified PolyPole-2 by comparing the results to a reference finite difference solution over a large number of randomly generated op-

eration histories, including postulated RIA transients. The results demonstrate that PolyPole-2 solves the general PDE system with high accuracy in all considered situations. Also, computational times associated with PolyPole-2 are substantially lower than those of finite difference algorithms. Thus, PolyPole-2 can be applied to any fuel performance code to accurately compute intra-granular fission gas release during both operational conditions and fast transients.

The PolyPole-2 algorithm provides an accurate and computationally efficient solution of the general problem of intra-granular fission gas release during non-equilibrium trapping and resolution. Hence, it overcomes the quasi-stationary approximation and the concept of an effective diffusion coefficient. Currently, the PolyPole-2 algorithm is implemented in the BISON fuel performance code [49,69] and is also available as a stand-alone program.

The concept of PolyPole-2 not only provides a means to solve the mathematical problem considered in this paper but more in general, opens the possibility to calculate intra-granular fission gas release in fuel performance codes according to systems of coupled PDEs. The algorithm can be adapted to solving more general formulations, for instance, including terms for bubble motion and/or nucleation. Although reducing these more general problems also to a single diffusion equation with an effective diffusion coefficient may be possible for specific cases (e.g., [58,70]), in general, coupled PDEs need to be considered explicitly. Application of the concept to increasingly complex formulations is of interest in perspective.

Acknowledgments

This work was supported at Idaho National Laboratory by the U.S. Department of Energy Scientific Discovery through Advanced Computing (SciDAC) project on Simulation of Fission Gas, the Nuclear Energy Advanced Modeling and Simulation (NEAMS) program and the Consortium for Advanced Simulation of Light Water Reactors (CASL). Support at JRC-Karlsruhe by the GENTLE Project 198236 is also acknowledged. This research contributes to

the U.S.-EURATOM International Nuclear Energy Research Initiative (INERI) project 2017-004-E on Modeling of Fission Gas Behavior in Uranium Oxide Nuclear Fuel Applied to Engineering Fuel Performance Codes. The work is also part of the R&D activities carried out by POLIMI in the framework of the IAEA Coordinated Research Project FUMAC (CRP-T12028, Fuel Modelling under Accident Conditions) and it contributes to the Joint Programme on Nuclear Materials (JPNM) of the European Energy Research Alliance (EERA), in the specific framework of the COMBATFUEL Project.

The authors are grateful to Prof. Klaus Lassmann for his review of the work and valuable advice, and to Charles Folsom (INL) for his help in the definition of the numerical experiment.

Data availability

The data generated during the current study are available from the corresponding author on request.

References

[1] J. Spino, J. Rest, W. Goll, C.T. Walker, Matrix swelling rate and cavity volume balance of UO_2 fuels at high burn-up, Journal of Nuclear Materials 346 (2005) 131–144.

[2] T. Tverberg, The high burn-up disk irradiation test, IFA-655: Final report on the in-pile performance, Tech. Rep. HWR-837, Halden Reactor Project (2008).

[3] P. Blair, Modelling of fission gas behaviour in high burnup nuclear fuel, Ph.D. thesis, École Polytechnique Fédérale de Lausanne, Switzerland (2008).

[4] V.V. Rondinella, T. Wiss, The high burn-up structure in nuclear fuel, Materials Today 13 (2010) 24–32.

[5] F. Cappia, D. Pizzocri, A. Schubert, P. Van Uffelen, G. Paperini, D. Pellottiero, R. Macián-Juan, V.V. Rondinella, Critical assessment of the pore size distribution in the rim region of high burnup UO_2 fuels, Journal of Nuclear Materials 480 (2016) 138–149.

[6] F. Schmitz, J. Papin, High burnup effects on fuel behaviour under accident conditions: the tests CABRI REP-Na, Journal of Nuclear Materials 270 (1999) 55–64.

[7] Y. Guerin, J. Noirot, D. Lespiaux, G. Chaigne, C. Blanpain, Microstructure evolution and in-reactor behavior of MOX fuel, in: Proc. of the ANS Int. Topical Meeting on LWR Fuel Performance, Park City, USA, April 10–13, 2000.

[8] F. Lemoine, B. Cazalis, H. Rigat, The role of fission gases on the high burn-up fuel behaviour in reactivity initiated accident conditions, in: Proc. of the 10^{th} Int. Symp. on Thermodynamics of Nuclear Materials, Halifax, Canada, August 6–11, 2000.

[9] J. Noirot, L. Desgranges, J. Lamontagne, Detailed characterisations of high burn-up structures in oxide fuels, Journal of Nuclear Materials 372 (2008) 318–339.

[10] T. Nakamura, H. Sasajima, T. Fuketa, K. Ishijima, Fission gas induced cladding deformation of LWR fuel rods under reactivity initiated accident conditions, Journal of Nuclear Science and Technology 33 (12) (1996) 924–935.

[11] F. Lemoine, High burnup fuel behavior related to fission gas effects under reactivity initiated accidents (RIA) conditions, Journal of Nuclear Materials 248 (1997) 238–248.

[12] P. Van Uffelen, M. Sheindlin, V. Rondinella, C. Ronchi, On the relations between the fission gas behaviour and the pellet-cladding mechanical interaction in LWR fuel rods, in: Proc. of the International Seminar on Pellet-Clad Interaction in Water Reactor Fuels, Aix-en-Provence, France, March 9–11, 2004.

[13] Standard review plan for the review of safety analysis reports for nuclear power plants, LWR edition, Tech. Rep. NUREG-0800, Section 4.2 Fuel System Design, Rev. 3, U.S. Nuclear Regulatory Commission, Office of Nuclear Reactor Regulation (2007).

[14] Fuel reliability program: Proposed reactivity insertion accident (RIA) acceptance criteria, revision 1, Tech. Rep. EPRI 3002005540, Electric Power Research Institute (2015).

[15] J. Desquines, D.A. Koss, A.T. Motta, B. Cazalis, M. Petit, The issue of stress state during mechanical tests to assess cladding performance during a reactivity-initiated accident (RIA), Journal of Nuclear Materials 412 (2011) 250–267.

[16] J.A. Turnbull, M.O. Tucker, Swelling in UO_2 under conditions of gas release, Philosophical Magazine 30 (1974) 47–63.

[17] K. Forsberg, A.R. Massih, Diffusion theory of fission gas migration in irradiated nuclear fuel UO_2, Journal of Nuclear Materials 135 (1985) 140–148.

[18] R.J. White, M.O. Tucker, A new fission-gas release model, Journal of Nuclear Materials 118 (1983) 1–38.

[19] T. Kogai, Modelling of fission gas release and gaseous swelling of light water reactor fuels, Journal of Nuclear Materials 244 (1997) 131–140.

[20] P. Van Uffelen, Contribution to the modelling of fission gas release in light water reactor fuel, Ph.D. thesis, University of Liège, Belgium (2002).

[21] R.J. White, The development of grain-face porosity in irradiated oxide fuel, Journal of Nuclear Materials 325 (2004) 61–77.

[22] M.S. Veshchunov, V.D. Ozrin, V.E. Shestak, V.I. Tarasov, R. Dubourg, G. Nicaise, Development of the mechanistic code MFPR for modelling fission-product release from irradiated UO_2 fuel, Nuclear Engineering and Design 236 (2006) 179–200.

[23] G. Pastore, L. Luzzi, V. Di Marcello, P. Van Uffelen, Physics-based modelling of fission gas swelling and release in UO_2 applied to integral fuel rod analysis, Nuclear Engineering and Design 256 (2013) 75–86.

[24] P. Blair, A. Romano, C. Hellwig, R. Chawla, Calculations on fission gas behaviour in the high burnup structure, Journal of Nuclear Materials 350 (2006) 232–239.

[25] Nuclear fuel behaviour under reactivity-initiated accident (RIA) conditions. State-of-the-art report, Tech. Rep. NEA/CSNI/R(2010)1, OECD/NEA (2010).

[26] Fuel modelling at extended burnup (FUMEX-II), Tech. Rep. IAEA-TECDOC-1687, International Atomic Energy Agency (2012).

[27] Improvement of computer codes used for fuel behaviour simulations (FUMEX-III), Tech. Rep. IAEA-TECDOC-1697 (2013).

[28] L. Holt, A. Schubert, J. van de Laar, P. Van Uffelen, Stand-alone modelling of the high burnup structure formation and burst release during design basis accidents, in: Proc. of the Enlarged Halden Programme Group Meeting, Røros, Norway, September 7–12, 2014.

[29] D. Pizzocri, F. Cappia, L. Luzzi, G. Pastore, V. Rondinella, P. Van Uffelen, A semi-empirical model for the formation and depletion of the high burnup structure in UO_2, Journal of Nuclear Materials 487 (2017) 23–29.

[30] M.V. Speight, A calculation on the migration of fission gas in material exhibiting precipitation and re-solution of gas atoms under irradiation, Nuclear Science and Engineering 37 (1969) 180–185.

[31] D.R. Olander, Fundamental Aspects of Nuclear Reactor Fuel Elements, Technical Information Center – Energy Research and Development Administration, University of California, Berkeley, CA, USA, 1976.

[32] P. Lösönen, On the behaviour of intragranular fission gas in UO_2 fuel, Journal of Nuclear Materials 280 (2000) 56–72.

[33] P. Van Uffelen, R.J.M. Konings, C. Vitanza, J. Tulenko, Analysis of reactor fuel rod behavior, in: D.G. Cacuci (Ed.), Handbook of Nuclear Engineering, Vol. 13, Springer Science + Business Media, LLC., New York, NY, USA, 2010, pp. 1519–1627.

[34] H. Matzke, Gas release mechanisms in UO_2 – a critical review, Radiation Effects 53 (1980) 219–242.

[35] J.A. Turnbull, C.A. Friskney, J.R. Findlay, F.A. Johnson, A.J. Walter, The diffusion coefficients of gaseous and volatile species during the irradiation of uranium dioxide, Journal of Nuclear Materials 107 (1982) 168–184.

[36] K. Lassmann, The structure of fuel element codes, Nuclear Engineering and Design 57 (1980) 17–39.

[37] P.T. Elton, K. Lassmann, Calculational methods for diffusional gas release, Nuclear Engineering and Design 101 (1987) 259–265.

[38] J.R. Matthews, M.H. Wood, An efficient method for calculating diffusive flow to a spherical boundary, Nuclear Engineering and Design 56 (1980) 439–443.

[39] L. Väth, Approximate treatment of the grain-boundary loss term in fission gas release models, Journal of Nuclear Materials 99 (1981) 324–325.

[40] K. Forsberg, A.R. Massih, Fission gas release under time-varying conditions, Journal of Nuclear Materials 127 (1985) 141–145.

[41] K. Lassmann, H. Benk, Numerical algorithms for intragranular fission gas release, Journal of Nuclear Materials 280 (2000) 127–135.

[42] P. Lösönen, Methods for calculating diffusional gas release from spherical grains, Nuclear Engineering and Design 196 (2000) 161–173.

[43] P. Hermansonn, A.R. Massih, An effective method for calculation of diffusive flow in spherical grains, Journal of Nuclear Materials 304 (2002) 204–211.

[44] J.-S. Cheon, Y.-H. Koo, B.-H. Lee, J.-Y. Oh, D.-S. Sohn, A two-zone method with an enhanced accuracy for a numerical solution of the diffusion equation, Journal of Nuclear Materials 359 (2006) 139–149.

[45] D. Pizzocri, C. Rabiti, L. Luzzi, T. Barani, P. Van Uffelen, G. Pastore, PolyPole-1: An accurate numerical algorithm for intra-granular fission gas release, Journal of Nuclear Materials 478 (2016) 333–342.

[46] Y. Rashid, R. Dunham, R. Montgomery, Fuel Analysis and Licensing Code: FALCON MOD01 – Volume 1: Theoretical and Numerical Bases, Tech. Rep. EPRI-1011307 (2004).

[47] M. Suzuki, H. Saitou, Y. Udagawa, F. Nagase, Light Water Reactor Fuel Analysis Code FEMAXI-7; Model and Structure, Tech. Rep. JAEA-data/code 2013-005 (2013).

[48] K. Lassmann, A. Schubert, P. Van Uffelen, C. Györi, J. van de Laar, TRANSURANUS Handbook, Copyright ©1975–2014, Institute for Transuranium Elements, Karlsruhe, Germany, 2014.

[49] J.D. Hales, R.L. Williamson, S.R. Novascone, G. Pastore, .W. Spencer, D.S. Stafford, K.A. Gamble, D.M. Perez, R.J. Gardner, W. Liu, BISON

Theory Manual: The Equations behind Nuclear Fuel Analysis, Tech. Rep. INL/EXT1329930, Rev. 1, Idaho National Laboratory (2015).

[50] K. Geelhood, W. Luscher, P. Raynaud, I. Porter, FRAPCON-4.0: A Computer Code for the Calculation of Steady-state, Thermal-Mechanical Behavior of Oxide Fuel Rods for High Burnup, Tech. Rep. PNNL-19418, Vol. 1, Rev.2, Pacific Northwest National Laboratory, USA (2015).

[51] M.S. Veshchunov, V. Tarasov, Modelling of irradiated UO_2 fuel behaviour under transient conditions, Journal of Nuclear Materials 437 (2013) 250–260.

[52] F.S. Ham, Theory of diffusion-limited precipitation, Journal of Physics and Chemistry of Solids 6 (1958) 335–351.

[53] R.S. Nelson, The stability of gas bubbles in an irradiation environment, Journal of Nuclear Materials 31 (1969) 153–161.

[54] J.A. Turnbull, The distribution of intragranular fission gas bubbles in UO_2 during irradiation, Journal of Nuclear Materials 38 (1971) 203–212.

[55] J.A. Turnbull, A review of irradiation induced re-solution in oxide fuels, Radiation Effects 53 (1980) 243–249.

[56] D.R. Olander, D. Wongsawaeng, Re-solution of fission gas – A review: Part I. Intragranular bubbles, Journal of Nuclear Materials 354 (2006) 94–109.

[57] J. Rest, An improved model for fission product behavior in nuclear fuel under normal and accident conditions, Journal of Nuclear Materials 120 (1984) 195–212.

[58] P. Van Uffelen, G. Pastore, V. Di Marcello, L. Luzzi, Multiscale modelling for the fission gas behavior in the TRANSURANUS code, Nuclear Engineering and Technology 43 (6) (2011) 477–488.

[59] D. Pizzocri, G. Pastore, T. Barani, A. Magni, L. Luzzi, P. Van Uffelen, S.A. Pitts, A. Alfonsi, J.D. Hales, A model describing intra-granular fission gas

behaviour in oxide fuel for advanced engineering tools, Journal of Nuclear Materials 502 (2018) 323–330.

[60] B.D. Wirth, Multiscale modeling of fission gas bubble evolution in UO_2 under nominal operating conditions, in: OECD/NEA workshop on nuclear-fuel modelling to support safety and performance ehancement for water-cooled reactors, Paris, France, March 7–9, 2017.

[61] A.H. Booth, A method of calculating gas diffusion from UO_2 fuel and its application to the X-2-f loop test, Tech. Rep. AECL-496, Atomic Energy of Canada Ltd. (1957).

[62] J. Papin, B. Cazalis, J. Frizonnet, J. Desquines, F. Lemoine, V. Georgenthum, F. Lamare, M. Petit, Summary and interpretation of the CABRI REP-Na program, Nuclear Technology 157 (2007) 230–250.

[63] C. Rabiti, Modelling of fast neutron transients in an accelerator driven system, Ph.D. thesis, Institut für Kernenergetik und Energiesysteme der Universität Stuttgart, Germany (2007).

[64] L.O. Jernkvist, Sensitivity Study on Clad Tube Failure under Reactivity Initiated Accidents in Light Water Reactors, Tech. Rep. SKI 2004:34, Swedish Nuclear Power Inspectorate (2004).

[65] K. Terrani, C. Parish, T. Gerczak, P. Edmondson, C. Baldwin, Advanced electron microscopy characterization of high burnup structure, in: Enlarged Halden Programme Group Meeting, Fornebu, Norway, May 8–13, 2016.

[66] I.L.F. Ray, H. Matzke, H.A. Thiele, M. Kinoshita, An electron microscopy study of the RIM structure of a UO_2 fuel with a high burnup of 7.9% FIMA, Journal of Nuclear Materials 245 (1997) 115–123.

[67] T. Sonoda, M. Kinoshita, I.L.F. Ray, T. Wiss, H. Thiele, D. Pellottiero, V.V. Rondinella, H. Matzke, Transmission electron microscopy observation on irradiation-induced microstructural evolution in high burn-up UO_2 disk

fuel, Nuclear Instruments and Methods in Physics Research B 191 (2002) 622–628.

[68] S. Brémier, C.T. Walker, Radiation-enhanced diffusion and fission gas release from recrystallised grains in high burn-up UO_2 nuclear fuel, Radiation Effects and Defects in Solids 157 (2002) 311–322.

[69] R.L. Williamson, J.D. Hales, S.R. Novascone, M.R. Tonks, D.R. Gaston, C.J. Permann, D. Andrs, R.C. Martineau, Multidimensional multiphysics simulation of nuclear fuel behavior, Journal of Nuclear Materials 423 (2012) 149–163.

[70] M.H. Wood, J.R. Matthews, A simple operational gas release and swelling model, Journal of Nuclear Materials 91 (1980) 35–40.

Appendix A

Analytic solution of the general system of PDEs for constant conditions

In this Appendix, we derive the analytic solution of Eqs. 1 for constant conditions and nonzero initial conditions. The considered mathematical problem is

$$\begin{cases} \frac{\partial c}{\partial t} = D\nabla^2 c - gc + bm + \beta \\ \frac{\partial m}{\partial t} = +gc \qquad - \qquad bm \end{cases} \tag{19}$$

where all symbols have been defined in Section 2.

We make the *ansatz* that $c(r,t)$ and $m(r,t)$ can be written as a linear combination of spatial modes

$$\begin{cases} c(r,t) = \sum_{k=1}^{\infty} x_k(t)\psi_k(r) \\ m(r,t) = \sum_{k=1}^{\infty} y_k(t)\psi_k(r) \end{cases} \tag{20}$$

where $\psi_k(r)$ are the spatial modes and $x_k(t)$ and $y_k(t)$ are the time coefficients.

Defining the vectors

$$u(r,t) = \begin{bmatrix} c(r,t) \\ m(r,t) \end{bmatrix} \tag{21}$$

and

$$z_k(t) = \begin{bmatrix} x_k(t) \\ y_k(t) \end{bmatrix} \tag{22}$$

Eq. 20 can be re-written in the form

$$u(r,t) = \sum_{k=1}^{\infty} z_k(t)\psi_k(r) \tag{23}$$

which makes evident that we are assuming the same spatial modes for both c and m. This vector notation is preferred in the rest of the manuscript (Section 4). In this Appendix, we adopt instead the notation of Eq. 20 for clarity.

Substituting Eqs. 20 into Eqs. 19 leads to

$$\begin{cases} \sum\limits_{k=1}^{\infty} \psi_k \frac{\partial x_k}{\partial t} = \sum\limits_{k=1}^{\infty} \left[x_k D\nabla^2\psi_k - g x_k \psi_k + b y_k \psi_k \right] + \beta \\ \sum\limits_{k=1}^{\infty} \psi_k \frac{\partial y_k}{\partial t} = \sum\limits_{k=1}^{\infty} \left[+g x_k \psi_k - b y_k \psi_k \right] \end{cases} \tag{24}$$

where time and space dependencies are omitted.

The spatial modes $\psi_k(r)$ are chosen as the eigenfunctions of the radial part of the spherical Laplacian, satisfying the Dirichlet boundary condition $(c,m)(r = a,t) = 0$ and the symmetry condition $\partial(c,m)/\partial r|_{r=0} = 0$, i.e., the normalized cardinal sines

$$\psi_k(r) = \frac{1}{\sqrt{2\pi a}} \frac{\sin(\lambda_k r)}{r} \tag{25}$$

with the eigenvalues

$$\lambda_k = \frac{k\pi}{a} \tag{26}$$

The eigenfunctions defined by Eq. 25 are orthonormal with respect to the scalar product

$$\langle \psi_n | \psi_k \rangle = \int_0^a 4\pi r^2 \psi_n \psi_k dr \tag{27}$$

Projecting Eqs. 24 on the spatial modes according to Eq. 27 results in

$$\begin{cases} \frac{dx_n}{dt} = -\delta_n x_n - g x_n + b y_n + \beta_n \\ \frac{dy_n}{dt} = +g x_n - b y_n \end{cases} \tag{28}$$

where $\delta_n = Dn^2\pi^2/a^2$ and $\beta_n = \langle \psi_n | \beta \rangle$. This a set of two linear first order differential equations. After defining the projected initial conditions as $(x_{n,0}, y_{n,0}) = \langle \psi_n | (c_0, m_0) \rangle$, Eqs. 28 can be solved via Laplace transform

$$\begin{cases} sX_n = x_{n,0} - \delta_n X_n - g X_n + b Y_n + \frac{\beta_n}{s} \\ sY_n = y_{n,0} + g X_n - b Y_n \end{cases} \tag{29}$$

where transformed variables are in capital letters. This algebraic system is solved for

$$\begin{aligned} X_n &= \frac{x_{n,0}s^2 + (bx_{n,0} + by_{n,0} + \beta_n)s + b\beta_n}{s[s^2 + (b + g + \delta_n)s + b\delta_n]} \\ Y_n &= \frac{y_{n,0}s^2 + (gx_{n,0} + gy_{n,0})s + g\beta_n}{s[s^2 + (b + g + \delta_n)s + b\delta_n]} \end{aligned} \tag{30}$$

The inverse transform of Eqs. 29 gives the solution of Eqs. 28 in the form

$$\begin{aligned} x_n(t) &= A_n \exp(-p_n t) + B_n \exp(-q_n t) + C_n \\ y_n(t) &= A'_n \exp(-p_n t) + B'_n \exp(-q_n t) + C'_n \end{aligned} \tag{31}$$

The solution of Eqs. 19 is obtained as linear combination of the spatial modes (Eq. 25) and the time coefficients (Eqs. 31)

$$\begin{cases} c(r,t) = \frac{1}{\sqrt{2\pi a}} \sum_{n=1}^{\infty} \frac{\sin(\lambda_n r)}{r} \left[A_n \exp(-p_n t) + B_n \exp(-q_n t) + C_n \right] \\ m(r,t) = \frac{1}{\sqrt{2\pi a}} \sum_{n=1}^{\infty} \frac{\sin(\lambda_n r)}{r} \left[A'_n \exp(-p_n t) + B'_n \exp(-q_n t) + C'_n \right] \end{cases} \tag{32}$$

which is the solution in spherical geometry for constant conditions of the general system of PDEs for intra-granular fission gas release. The expressions for the coefficients and for the poles of Eqs. 31 are given in Table 1.

We define the spatially averaged concentrations in the grain as

$$(\bar{c}(t), \bar{m}(t)) = \frac{\int_0^a 4\pi r^2 \, (c(r,t), m(r,t)) \, dr}{\frac{4}{3}\pi a^3} \tag{33}$$

Integrating Eqs. 32 according to Eq. 33 we obtain the spatially averaged solution

$$\begin{aligned}
\bar{c}(t) \quad &= \tfrac{\beta a^2}{15D}\left[1 + \tfrac{90}{\pi^4}\sum_{n=1}^{\infty}\tfrac{1}{n^4}\left(\tfrac{q_n}{b}\tfrac{b-p_n}{p_n-q_n}\exp(-p_n t) + \tfrac{p_n}{b}\tfrac{b-q_n}{q_n-p_n}\exp(-q_n t)\right)\right] \\
&+ c_0 \tfrac{6}{\pi^2}\sum_{n=1}^{\infty}\tfrac{1}{n^2}\left(-\tfrac{b-p_n}{p_n-q_n}\exp(-p_n t) + \tfrac{b-q_n}{q_n-p_n}\exp(-q_n t)\right) \\
&+ m_0 \tfrac{6}{\pi^2}\sum_{n=1}^{\infty}\tfrac{1}{n^2}\left(-\tfrac{b}{p_n-q_n}\exp(-p_n t) + \tfrac{b}{p_n-q_n}\exp(-q_n t)\right)
\end{aligned}$$

$$\begin{aligned}
\bar{m}(t) \quad &= \tfrac{\beta a^2}{15D}\tfrac{g}{b}\left[1 + \tfrac{90}{\pi^4}\sum_{n=1}^{\infty}\tfrac{1}{n^4}\left(\tfrac{q_n}{p_n-q_n}\exp(-p_n t) + \tfrac{p_n}{q_n-p_n}\exp(-q_n t)\right)\right] \\
&+ c_0 \tfrac{6}{\pi^2}\sum_{n=1}^{\infty}\tfrac{1}{n^2}\left(-\tfrac{g}{p_n-q_n}\exp(-p_n t) - \tfrac{g}{q_n-p_n}\exp(-q_n t)\right) \\
&+ m_0 \tfrac{6}{\pi^2}\sum_{n=1}^{\infty}\tfrac{1}{n^2}\left(\tfrac{b-q_n}{p_n-q_n}\exp(-p_n t) + \tfrac{b-p_n}{q_n-p_n}\exp(-q_n t)\right)
\end{aligned} \tag{34}$$

Appendix B

Derivation of Speight's formulation

In this Appendix, we derive Speight's formulation for the problem of intra-granular fission gas release in presence of trapping and resolution. Following a slightly different procedure than Speight's [30], we demonstrate that the solution of the general problem (Appendix A) reduces to the solution of a single diffusion equation with an effective diffusion coefficient (Eq. 8), under the same assumptions applied by Speight. Note that, while Speight limited his derivation to the case of zero initial conditions for the gas concentration, we deal with the more general case of nonzero initial conditions.

Like Speight's, our procedure is based on the analytic solution of the general problem for constant conditions. We seek the solution in terms of the total concentration of intra-granular gas, $c_t = c + m$. Also, we consider the spatially

Table 1: Expressions for the coefficients and poles in the solution of the general system of PDEs for constant conditions, Eq. 32.

Parameter	Expression
p_n	$\frac{1}{2}\left[(b+g+\delta_n)+\sqrt{(b+g+\delta_n)^2-4b\delta_n}\right]$
q_n	$\frac{1}{2}\left[(b+g+\delta_n)-\sqrt{(b+g+\delta_n)^2-4b\delta_n}\right]$
A_n	$\frac{1}{p_n-q_n}\left[(b-q_n)x_{n,0}+by_{n,0}+\frac{\beta_n}{\delta_n}q_n\right]$
B_n	$\frac{1}{p_n-q_n}\left[(b-p_n)x_{n,0}+by_{n,0}+\frac{\beta_n}{\delta_n}p_n\right]$
C_n	$\frac{\beta_n}{\delta_n}$
A'_n	$\frac{1}{p_n-q_n}\left[gx_{n,0}+(g-q_n+\delta_n)y_{n,0}+\frac{\beta_n}{\delta_n}\frac{g}{b}q_n\right]$
B'_n	$\frac{1}{p_n-q_n}\left[gx_{n,0}+(g-p_n+\delta_n)y_{n,0}+\frac{\beta_n}{\delta_n}\frac{g}{b}p_n\right]$
C'_n	$\frac{\beta_n}{\delta_n}\frac{g}{b}$

averaged concentrations in the grain. Summation of Eqs. 34 yields for the total concentration

$$
\begin{aligned}
&\bar{c}_t(t) = (\bar{c}+\bar{m})(t) = \\
&= \frac{\beta a^2}{15D}\left[1+\frac{g}{b}+\frac{90}{\pi^4}\sum_{n=1}^{\infty}\frac{1}{n^4}\left(\frac{q_n}{b}\frac{b-p_n}{p_n-q_n}+\frac{g}{b}\frac{q_n}{p_n-q_n}\right)\exp(-p_nt)\right]+ \\
&+\frac{\beta a^2}{15D}\left[\frac{90}{\pi^4}\sum_{n=1}^{\infty}\frac{1}{n^4}\left(\frac{p_n}{b}\frac{b-q_n}{q_n-p_n}+\frac{g}{b}\frac{p_n}{q_n-p_n}\right)\exp(-q_nt)\right]+ \\
&+c_0\frac{6}{\pi^2}\sum_{n=1}^{\infty}\frac{1}{n^2}\left(-\frac{b-p_n}{p_n-q_n}-\frac{g}{p_n-q_n}\right)\exp(-p_nt)+ \\
&+c_0\frac{6}{\pi^2}\sum_{n=1}^{\infty}\frac{1}{n^2}\left(-\frac{b-q_n}{q_n-p_n}-\frac{g}{q_n-p_n}\right)\exp(-q_nt)+ \\
&+m_0\frac{6}{\pi^2}\sum_{n=1}^{\infty}\frac{1}{n^2}\left(-\frac{b}{p_n-q_n}+\frac{b-q_n}{p_n-q_n}\right)\exp(-p_nt)+ \\
&+m_0\frac{6}{\pi^2}\sum_{n=1}^{\infty}\frac{1}{n^2}\left(\frac{b}{p_n-q_n}+\frac{b-p_n}{q_n-p_n}\right)\exp(-q_nt)
\end{aligned}
\tag{35}
$$

In line with Speight, we apply the assumption that trapping and resolution

act on a smaller time scale than diffusion, i.e., a fission gas atom will experience, on average, many trapping and resolution events at bubbles before reaching the grain boundary. This can be expressed as

$$b + g >> \delta_n = Dn^2\pi^2/a^2 \tag{36}$$

Clearly, the hypothesis expressed by Eq. 36 holds only for modes $n < n_0$, with n_0 being a finite number. In the following, we derive the approximate solution of the problem applying Eq. 36, then we show *a posteriori* that the formulation holds with $n < n_0$ under a further hypothesis applied to time t. Such further hypothesis also is analogous to that proposed by Speight.

Under the hypothesis expressed by Eq. 36, the expression for the poles q_n of the system (Table 1)

$$q_n = \frac{1}{2}\left[(b + g + \delta_n) - \sqrt{(b + g + \delta_n)^2 - 4b\delta_n}\right] \tag{37}$$

can be simplified as follows

$$\begin{aligned} q_n &\approx \frac{1}{2}\left[(b + g) - \sqrt{(b + g)^2 - 4b\delta_n}\right] = \\ &= \frac{1}{2}(b + g)\left[1 - \sqrt{1 - \frac{4b\delta_n}{(b + g)^2}}\right] \simeq \\ &\simeq \frac{1}{2}(b + g)\left[1 - \left(1 - \frac{2b\delta_n}{(b + g)^2}\right)\right] = \\ &= \frac{b}{b + g}\delta_n \end{aligned} \tag{38}$$

Consider also the following approximations in the pre-exponential factors in

Eq. 35

$$
\begin{aligned}
&\frac{q_n}{b}\frac{b-p_n}{p_n-q_n}+\frac{g}{b}\frac{q_n}{p_n-q_n}\approx\frac{(b+g)\dfrac{b}{b+g}\delta_n-b\delta_n}{b\left(b+g-\dfrac{b}{b+g}\delta_n\right)}=0\\
&\frac{p_n}{b}\frac{b-q_n}{q_n-p_n}+\frac{g}{b}\frac{p_n}{q_n-p_n}\approx\frac{(b+g)^2-b\delta_n}{b\left(\dfrac{b}{b+g}\delta_n-(b+g)\right)}\approx-\frac{b+g}{b}\\
&-\frac{b-p_n}{p_n-q_n}-\frac{g}{q_n-p_n}\approx-\frac{(b+g)-(b+g)}{b+g-\dfrac{b}{b+g}\delta_n}=0\\
&-\frac{b-q_n}{q_n-p_n}-\frac{g}{q_n-p_n}\approx-\frac{b+g-\dfrac{b}{b+g}\delta_n}{\dfrac{b}{b+g}\delta_n-(b+g)}=+1\\
&-\frac{b}{p_n-q_n}+\frac{b-q_n}{p_n-q_n}\approx\frac{-b+b-\dfrac{b}{b+g}\delta_n}{b+g-\dfrac{b}{b+g}\delta_n}\approx0\\
&\frac{b}{p_n-q_n}+\frac{b-p_n}{q_n-p_n}\approx\frac{-b+b-(b+g)}{\dfrac{b}{b+g}\delta_n-(b+g)}\approx+1
\end{aligned}
\tag{39}
$$

Substituting Eqs. 38 and 39 into Eq. 35, one gets

$$
\begin{aligned}
&\bar{c}_t(t)\approx c_{t_0}\frac{6}{\pi^2}\sum_{n=1}^{\infty}\frac{1}{n^2}\exp\left(-\frac{b}{b+g}\delta_n t\right)+\\
&+\frac{\beta a^2}{15D}\frac{b+g}{b}\left[1-\frac{90}{\pi^4}\sum_{n=1}^{\infty}\frac{1}{n^4}\exp\left(-\frac{b}{b+g}\delta_n t\right)\right]
\end{aligned}
\tag{40}
$$

After successive terms in the summations, the exponentials assume a value which is negligible with respect to unity for values of $n > n_0$ such that

$$
\frac{b}{b+g}\delta_{n_0}t=q_{n_0}t=\frac{Db{n_0}^2\pi^2}{a^2\,(b+g)}t\approx5 \tag{41}
$$

and the hypothesis expressed by Eq. 36 becomes, by substitution,

$$
bt >> 5 \tag{42}
$$

which is the time condition under which Eq. 36 holds, as also shown in [30].

Under the condition expressed by Eq. 41, Eq. 40 becomes

$$\bar{c}_t(t) \approx c_{t_0} \frac{6}{\pi^2} \sum_{n=1}^{n_0} \frac{1}{n^2} \exp\left(-\frac{b}{b+g}\delta_n t\right) + \\ + \frac{\beta a^2}{15D} \frac{b+g}{b} \left[1 - \frac{90}{\pi^4} \sum_{n=1}^{n_0} \frac{1}{n^4} \exp\left(-\frac{b}{b+g}\delta_n t\right)\right] \tag{43}$$

As demonstrated in [45], Eq. 43 can be obtained as the truncation of the spatially averaged solution of the following equation

$$\frac{\partial c_t}{\partial t} = \frac{b}{b+g} D \nabla^2 c_t + \beta \tag{44}$$

Equation 44 can be written as

$$\frac{\partial c_t}{\partial t} = D_{eff} \nabla^2 c_t + \beta \tag{45}$$

which corresponds to Eq. 8. $D_{eff} = b/(b+g)\ D$ is the effective diffusion coefficient of Speight [30]. Hence, as previously demonstrated by Speight, under the applied assumptions the problem of intra-granular fission gas release reduces to an expression (Eq. 45) formally analogous to the formulation of Booth [61] for the case of diffusion of single gas atoms in the absence of trapping and resolution, with a reduced (effective) diffusion coefficient.